

Thomson Scattering Measurement of Laser-Produced Plasma in a Magnetic Thrust Chamber

Yutaro ITADANI, Taichi MORITA¹⁾, Naoya SAITO, Masafumi EDAMOTO, Tomihiko KOJIMA, Mariko TAKAGI²⁾, Keisuke NAGASHIMA²⁾, Shinsuke FUJIOKA³⁾, Akifumi YOGO³⁾, Hiroaki NISHIMURA³⁾, Atushi SUNAHARA⁴⁾, Yoshitaka MORI⁵⁾, Tomoyuki JOHZAKI⁶⁾, Hideki NAKASHIMA¹⁾ and Naoji YAMAMOTO¹⁾

Interdisciplinary Graduate School of Engineering Sciences, Kyushu University, Kasuga 826-8550, Japan

¹⁾*Faculty of Engineering Sciences, Kyushu University, Kasuga 826-8550, Japan*

²⁾*Faculty of Engineering, Kyushu University, 744 Motoooka, Nishi-ku, Fukuoka 819-0395, Japan*

³⁾*Institute of Laser Engineering, Osaka University, Suita 565-0871, Japan*

⁴⁾*Center for Materials Under Extreme Environment, School of Nuclear Engineering, Purdue University, West Lafayette, Indiana 47907, USA*

⁵⁾*The Graduate School for the Creation of New Photonics Industries, Hamamatsu 431-1202, Japan*

⁶⁾*Hiroshima University, Higashi Hiroshima 739-0046, Japan*

(Received 19 December 2017 / Accepted 13 February 2018)

Laser fusion rocket is one of the candidate propulsion devices for Mars exploration. It obtains thrust from the interaction between plasma and magnetic field and this propulsion system is called magnetic thrust chamber. We constructed a spectrometer with high wavelength resolution of 35 pm to obtain plasma parameters by measuring ion feature of laser Thomson scattering from a laser-produced plasma in a magnetic thrust chamber. We obtain the plasma parameters such as electron temperature, electron density, and velocity as well as the plasma density structure showing the stagnation of the plasma by magnetic field.

© 2018 The Japan Society of Plasma Science and Nuclear Fusion Research

Keywords: Thomson scattering, laser fusion rocket, magnetic thrust chamber, high-power laser, ablation plasma

DOI: 10.1585/pfr.13.1306016

These days Mars explorations have been planned in United states and China etc. Round trip to Mars requires about 500 days with a chemical rocket. This long mission time causes physical and the mental damages on astronauts. To reduce the mission period, laser fusion rocket (LFR) has been proposed as one of the candidates. LFR obtains thrust from the interaction between plasma and magnetic field, and it reuses a part of fusion energy to drive a laser system. LFR generates large thrust with low fuel consumption, and the mission period will be reduced to 135 days [1, 2].

The propulsion system of LFR is called as magnetic thrust chamber. Figure 1 shows a mechanism of the thrust generation in a magnetic thrust chamber. A fusion plasma is generated by inertial confinement fusion in an external magnetic field applied by an electromagnetic coil (Fig. 1 (a)). A diamagnetic cavity is formed in the plasma and the plasma compresses the magnetic field outside (Fig. 1 (b)). Finally, the compressed magnetic field pushes back the plasma and LFR is accelerated by a reaction force (Fig. 1 (c)).

A conceptual design of LFR has been proposed by Orth [3]. However, its propulsion system and plasma pa-

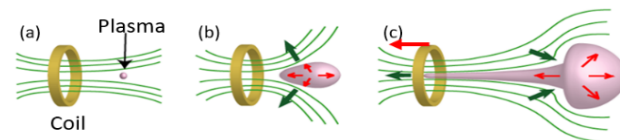


Fig. 1 The mechanism of thrust generation in a magnetic thrust chamber.

rameters in a magnetic thrust chamber have not been studied sufficiently. We have done some experiments in order to demonstrate the propulsion system at Institute of Laser Engineering (ILE), Osaka University. In the previous studies, thrust has been measured directly using a thrust stand [1] and the electron density distribution in the thrust system has been measured with Mach-Zehnder interferometer [4]. However, plasma parameters: temperature velocity, and charge state have never been measured in spite of its importance in the comparison between experiments and numerical simulations. Therefore, we establish a measurement system available in a magnetic thrust chamber by using collective Thomson scattering technique.

The experiment used Gekko XII (G XII) laser beams at ILE, to generate an ablation plasma instead of the fu-

author's e-mail: itadani@aes.kyushu-u.ac.jp

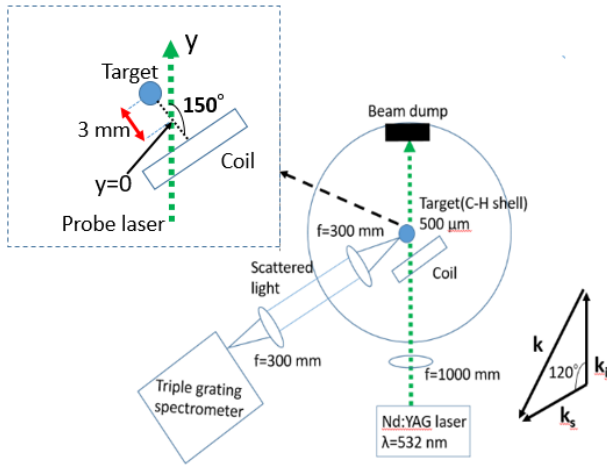


Fig. 2 Schematic of the experimental setup and Thomson scattering system.

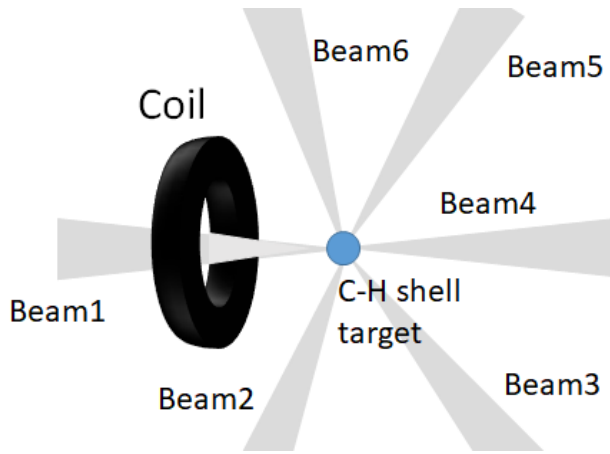


Fig. 3 Target irradiation by six beams.

sion plasma. Figure 2 shows the experimental setup. C-H shell target with a diameter of $500\ \mu\text{m}$ and thickness of $7\ \mu\text{m}$ placed in the center of a target chamber is irradiated by six beams (the energy of $25\ \text{J}/\text{beam}$) from six different angles as shown in Fig. 3 to generate an ablation plasma in a diverging magnetic field applied by an electromagnetic coil. The initial field strength at the target position is $0.7\ \text{T}$. After $100\ \text{ns}$ from the plasma generation, the second harmonic of the Nd: YAG laser (Continuum: Sure-Lite Ex, wavelength of $532\ \text{nm}$ and energy of $360\ \text{mJ}$) was injected at $3\ \text{mm}$ from the center of target chamber as a probe laser. Thomson scattered light was collected by a lens ($f = 300\ \text{mm}$) located at $300\ \text{mm}$ from the plasma, and was guided and focused to a spectrometer by another lens ($f = 300\ \text{mm}$). A beam dump was set at the exit window to prevent the reflection of the probe laser.

Laser Thomson scattering is used for measuring plasma parameters such as electron temperature, density, and drift velocity without disturbing the plasma [5, 6]. Thomson scattering shows two different regimes depend-

ing on the parameter $\alpha = 1/k\lambda_d$: collective ($\alpha > 1$) and non-collective ($\alpha \ll 1$). Here, setting the wavenumber vector of the incident laser as \mathbf{k}_i , and wavenumber vector of scattered light as \mathbf{k}_s , \mathbf{k} is defined by $\mathbf{k}_s - \mathbf{k}_i$ as shown in Fig. 2, where λ_d is Debye length. In this experiment, α is about 1.7 and it is in collective regime. The collective scattering is composed of ion and electron terms, and they have two peaks in wavelength which correspond to ion acoustic and electron plasma waves, respectively. The electron term is too weak to detect because of large self-emission in high-density laser-produced plasma, and we measured the ion term with narrower width and higher intensity. Because the ion term shows ion acoustic wave in the plasma, some parameters such as electron temperature T_e , ion temperature T_i , drift velocity v_k (velocity along \mathbf{k}), and electron density n_e are obtained. T_e and T_i are defined from the width of the spectrum, v_k is defined from the Doppler shift from the incident laser wavelength of $532\ \text{nm}$, and n_e is calculated comparing the Thomson scattering intensity with Rayleigh scattering intensity: $n_e = I_T \sigma_R n_0 / I_R \sigma_T S_i$, where I_T and I_R are the total scattering powers of Thomson and Rayleigh scatterings, respectively, σ_T and σ_R are the cross sections of Thomson and Rayleigh scattering, respectively, S_i is the total cross section of ion term and n_0 is the nitrogen density for Rayleigh scattering measurements [7]. We developed an additive dispersion spectrometer with three gratings [8] (Richardson gratings, $1800/\text{mm}$) to measure the ion term.

To calibrate wavelength of this spectrometer and to evaluate stray light, we measured Rayleigh and Raman scattering of the probe laser in the nitrogen filled chamber. The Rayleigh scattering spectrum was measured in some different pressure varying pressure from $0\ \text{Torr}$ to $100\ \text{Torr}$ with the probe laser energy of $28\ \text{mJ}$. Figure 4 (a) shows the Rayleigh scattering spectrum fitted with Gaussian. The wavelength is calibrated from Raman scattering and its value is $5.8\ \text{pm}/\text{pixel}$ (not shown). The full width at half maximum of Rayleigh spectrum becomes $46\ \text{pm}$. Figure 4 (b) shows the pressure dependence of Rayleigh scattering signal intensity. The Rayleigh scattering power is calculated from the integration of the signal along wavelength. From Fig. 4 (b), the stray light intensity in this measurement is estimated as 4.8, which is equal to the Rayleigh scattering in the pressure of $1.5\ \text{Torr}$, and is six times smaller than Thomson scattering intensity. Therefore, the stray light is small enough for Thomson scattering measurement.

Figure 5 (a) shows the Thomson scattering spectrum at $t = 100\ \text{ns}$. The vertical and horizontal axes show, respectively, the position along the probe laser and wavelength. The position at $y = 0$ is at $3\ \text{mm}$ from the center of the target chamber. The positive direction of y -axis is the incident direction of the probe laser.

The stray light observed at $\lambda \sim 532\ \text{nm}$ at $y > 1.4$ comes from the reflection of the probe laser at the target holder. Clear ion term of Thomson scattering is observed at $0.5\ \text{mm} < y < 1.1\ \text{mm}$. A broad spectrum in wave-

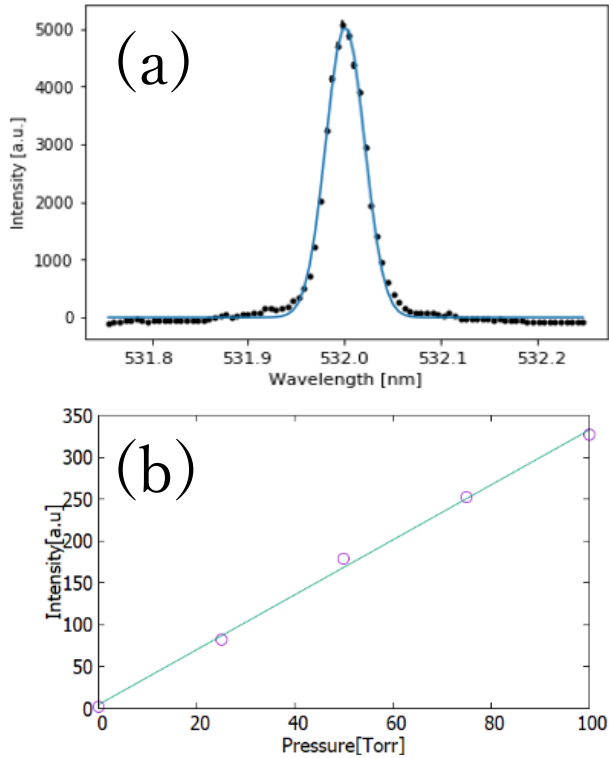


Fig. 4 (a) Fitting result of Rayleigh scattering and (b) pressure dependence of Rayleigh scattering signal intensity.

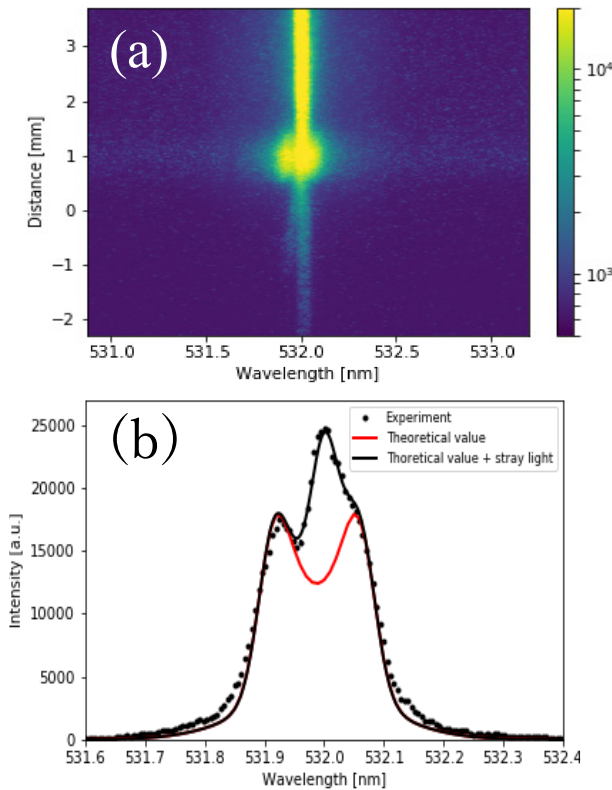


Fig. 5 (a) The Thomson spectrum of ablation plasma in a magnetic field of 0.7 T and (b) comparison of experimental value and theoretical curve.

length is observed at $y \sim 0.9$ mm. This spectrum shows the thermal bremsstrahlung emission, meaning high-density plasma exists because of the stagnation by the external magnetic field. This stagnation is also observed in the previous experiment measured by Mach-Zehnder interferometry [4].

Thomson scattering spectrum is also observed at $y \sim 0$ mm. This narrow spectrum shows that low temperature plasma exists near the coil axis without the stagnation because the magnetic field line in this region is quasi-parallel to the plasma expansion. The temperature and density of the plasma are estimated as $T_e \sim 4.1$ eV and $n_e \sim 2 \times 10^{17}$ cm $^{-3}$, respectively. In general, when plasmas stagnate, the temperature and density should increase due to the compression by the magnetic field. However, this plasma does not stagnate and the temperature and density do not rise.

The spectrum averaged with a width of 0.1 mm at $y = 0.9$ mm is plotted in Fig. 5 (b). Plasma parameters are obtained by comparing experimental values with theoretical function with two ion species i ($i = \text{H}$ for hydrogen and $i = \text{C}$ for carbon):

$$S(k, \lambda) = (2\pi/k) |\chi_e / \epsilon|^2 \sum_i (Z_i^2 n_i / n_e) f_{i0}((\omega + \mathbf{k} \cdot \mathbf{v}_d) / k),$$

where $\omega = \omega_s - \omega_0$, ω_s and ω_0 are the frequencies of scattered light and probe laser, respectively, n_i is the density of each ion species, v_d is the drift velocity, $\epsilon = 1 + \chi_e + \sum_i \chi_i$ is the dielectric function, χ_e and χ_i are electron and ion susceptibilities, respectively, f_{i0} is the ion velocity distribution function assuming Maxwell distribution here, and Z_i is the average charge state. Here, we assume that the carbon and hydrogen have the same temperature, density, composition, and drift velocity, and that the hydrogens are fully ionized. In Fig. 5 (b), experimental values and theoretical value are largely different near $\lambda = 532$ nm due to stray light. Assuming the stray light as Gaussian, electron temperature T_e is 18 ± 2.6 eV, electron density n_e is $(1.3 \pm 0.1) \times 10^{18}$ cm $^{-3}$ and velocity v_k is 4 km/s along \mathbf{k} direction. We measured the spectrum between the target and the coil, and the velocity component on \mathbf{k} vector in this region is basically positive and calculated as 15 km/s without magnetic field. However, we observed smaller velocity $v_k \sim 4$ km/s with the magnetic field. This means that the plasma is decelerated by the magnetic pressure.

Figures 6 (a) and 6 (b) show the spatial distributions of the electron temperature and electron density, respectively. Considering the error bar, the electron temperature is almost constant in the range of $y = 0.5$ mm to 1.1 mm. In this experiment, electron-ion collision time is about 2 ps using the typical plasma parameters, which is much smaller than the exposure time of the detector (~ 6 ns), and the electrons and ions can be isothermal in the region we observe. For this reason, it is considered that T_e and T_i are constant at $0.5 \text{ mm} < y < 1.1 \text{ mm}$ and the theoretical function is calculated assuming that $T_e = T_i$. On the other hand, the electron density changes depending on the posi-

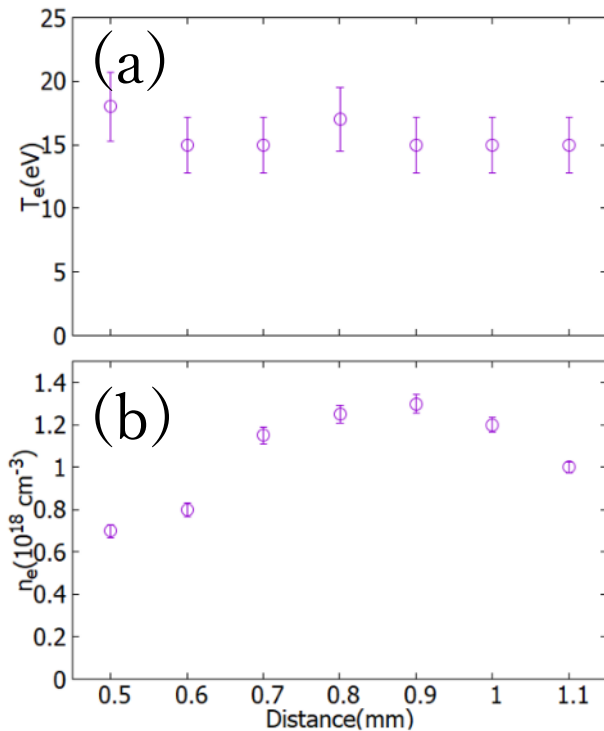


Fig. 6 (a) Electron temperature and (b) electron density of ablation plasma distribution.

tion. It takes a maximum value at 0.9 mm and it decreases as it approaches to 0.5 mm and 1.1 mm. The expanding plasma stagnates while the slower plasma catches up with the faster plasma around $y \sim 0.5$ mm, making large density jump at $y \sim 0.5$ mm. Also, the stagnation region even has larger temperature compared with low temperature plasma observed at $y \sim 0$ mm. The maximum value of the β at the stagnation region is estimated from the initial magnetic field and the plasma pressure, resulting in $\beta = 10$. In previous experiment, when the plasma expands in a magnetic field, it is confirmed that the magnetic field becomes

stronger [9]. For this reason, it is considered that β is less than 10.

In summary, we have conducted the Thomson scattering measurement in a magnetic thrust chamber. We obtained electron temperature, density, and velocity by fitting the spectrum with a theoretical function. The stagnation of the plasma by the magnetic field is observed as well. This stagnation was previously observed in density measurement [4]. This measurement system is useful to obtain plasma parameters such as electron and ion temperatures, electron density, and velocity, and also these results can be compared with numerical simulation we are now developing for future thrust system [10].

The authors would like to thank the dedicated technical support by the staff at the GEKKO-XII facility. This work was supported by JSPS KAKENHI grant number 15K18283 and 17K14876, and this work was performed under the joint research project of the Institute of Laser Engineering, Osaka University.

- [1] A. Maeno, N. Yamamoto and H. Nakashima, *J. Plasma Fusion Res.* **86**, 594 (2010).
- [2] H. Nakashima "Present Status of Nuclear Space Engine" Atomic Energy Society of Japan (2014).
- [3] C.D. Orth *et al.*, UCRL-LR-110500 (2003).
- [4] T. Morita *et al.*, *J. Phys.: Conference series* **717**, 012071 (2016).
- [5] K. Muraoka and M. Maeda, *Laser measurement of plasma and gas* (Industry books, 1995).
- [6] *Principles and Applications of Plasma Diagnostics*, ed. The Japan Society of Plasma Science and Nuclear Fusion Research (Corona publishing CO. LTD, 2006).
- [7] D.H. Froula *et al.*, *Plasma Scattering of Electromagnetic Radiation* (Academic Press, 2011).
- [8] K. Tomita and K. Uchino, *J. Plasma Fusion Res.* **89**, 664 (2013).
- [9] T. Morita *et al.*, *Scientific Reports* 10.1038/s41598-017-09273-3 (2017).
- [10] M. Edamoto *et al.*, 52nd AIAA/SAE/ASEE Joint Propulsion Conference 10.2514/6.2016-4684 (2016).